Published in final edited form as:
Eur J Nucl Med Mol Imaging. 2011 September ; 38(9): 1732–1741. doi:10.1007/s00259-011-1847-4.

One-step radiosynthesis of ^{18}F-AlF-NOTA-RGD$_2$ for tumor angiogenesis PET imaging

Shuanglong Liu,
Molecular Imaging Program at Stanford (MIPS), Canary Center at Stanford for Cancer Early Detection, Bio-X Program, Department of Radiology, Stanford University, 1201 Welch Road, Lucas Expansion, P095, Stanford, CA 94305-5344, USA

Hongguang Liu,
Molecular Imaging Program at Stanford (MIPS), Canary Center at Stanford for Cancer Early Detection, Bio-X Program, Department of Radiology, Stanford University, 1201 Welch Road, Lucas Expansion, P095, Stanford, CA 94305-5344, USA

Han Jiang,
Molecular Imaging Program at Stanford (MIPS), Canary Center at Stanford for Cancer Early Detection, Bio-X Program, Department of Radiology, Stanford University, 1201 Welch Road, Lucas Expansion, P095, Stanford, CA 94305-5344, USA. Department of Nuclear Medicine, Medical PET Center, Institute of Nuclear Medicine and Molecular Imaging, and the Second Affiliated Hospital of Zhejiang University School of Medicine, Key Laboratory of Medical Molecular Imaging of Zhejiang Province, Hangzhou, Zhejiang 310009, China

Yingding Xu,
Molecular Imaging Program at Stanford (MIPS), Canary Center at Stanford for Cancer Early Detection, Bio-X Program, Department of Radiology, Stanford University, 1201 Welch Road, Lucas Expansion, P095, Stanford, CA 94305-5344, USA

Hong Zhang, and
Department of Nuclear Medicine, Medical PET Center, Institute of Nuclear Medicine and Molecular Imaging, and the Second Affiliated Hospital of Zhejiang University School of Medicine, Key Laboratory of Medical Molecular Imaging of Zhejiang Province, Hangzhou, Zhejiang 310009, China

Zhen Cheng
Molecular Imaging Program at Stanford (MIPS), Canary Center at Stanford for Cancer Early Detection, Bio-X Program, Department of Radiology, Stanford University, 1201 Welch Road, Lucas Expansion, P095, Stanford, CA 94305-5344, USA

Zhen Cheng: zcheng@stanford.edu

Abstract

Correspondence to: Zhen Cheng, zcheng@stanford.edu.

Shuanglong Liu and Hongguang Liu contributed equally to the work.

Conflicts of interest None.

Purpose—One of the major obstacles of the clinical translation of ^{18}F-labeled arginine-glycine-aspartic acid (RGD) peptides has been the laborious multistep radiosynthesis. In order to facilitate the application of RGD-based positron emission tomography (PET) probes in the clinical setting we investigated in this study the feasibility of using the chelation reaction between Al^{18}F and a macrocyclic chelator-conjugated dimeric RGD peptide as a simple one-step ^{18}F labeling strategy for development of a PET probe for tumor angiogenesis imaging.

Methods—Dimeric cyclic peptide E[*c*(RGDyK)]$_2$ (RGD$_2$) was first conjugated with a macrocyclic chelator, 1,4,7-triazacyclononane-1,4,7-triacetic acid (NOTA), and the resulting bioconjugate NOTA-RGD$_2$ was then radiofluorinated via Al^{18}F intermediate to synthesize ^{18}F-AlF-NOTA-RGD$_2$. Integrin binding affinities of the peptides were assessed by a U87MG cell-based receptor binding assay using ^{125}I-echistatin as the radioligand. The tumor targeting efficacy and in vivo profile of ^{18}F-AlF-NOTA-RGD$_2$ were further evaluated in a subcutaneous U87MG glioblastoma xenograft model by microPET and biodistribution.

Results—NOTA-RGD$_2$ was successfully ^{18}F-fluorinated with good yield within 40 min using the Al^{18}F intermediate. The IC$_{50}$ of ^{19}F-AlF-NOTA-RGD$_2$ was determined to be 46±4.4 nM. Quantitative microPET studies demonstrated that ^{18}F-AlF-NOTA-RGD$_2$ showed high tumor uptake, fast clearance from the body, and good tumor to normal organ ratios.

Conclusion—NOTA-RGD$_2$ bioconjugate has been successfully prepared and labeled with Al^{18}F in one single step of radiosynthesis. The favorable in vivo performance and the short radiosynthetic route of ^{18}F-AlF-NOTA-RGD$_2$ warrant further optimization of the probe and the radiofluorination strategy to accelerate the clinical translation of ^{18}F-labeled RGD peptides.

Keywords

RGD dimer; ^{18}F; NOTA; PET; Aluminum fluoride; Molecular imaging; Integrin $\alpha_v\beta_3$

Introduction

Integrins are a family of transmembrane receptors, composed of 18 α and 8 β chains that can be combined to form 24 heterodimeric glycoproteins with distinct cellular and adhesive specificities. Among the integrin family, it has been well documented that integrin $\alpha_v\beta_3$ can elicit specific cell survival signals that facilitate vascular cell proliferation during angiogenesis but not in quiescent endothelium [1]. Integrin $\alpha_v\beta_3$ plays a vital role in the initiation, progression, and metastasis of many types of cancers [2–4]. Antagonists to integrins have been demonstrated to inhibit tumor angiogenesis, tumor growth, and metastasis in vivo [5]. Therefore, visualization and quantification of tumor integrin $\alpha_v\beta_3$ expression levels are critically important not only for the diagnosis and staging of cancer but also for the selection of patients for anti-integrin treatments and monitoring of treatment efficacy. Positron emission tomography (PET) is a powerful modality for noninvasive imaging of different molecular targets and events thanks to its high sensitivity, reasonable spatial resolution, and good quantification ability. Developing PET probes to monitor integrin expression has been one of the most extensively studied areas in molecular imaging.

Arginine-glycine-aspartic acid (RGD) is a conserved amino acid motif that widely exists in many extracellular matrix proteins that bind to integrins. A variety of RGD-based probes

have been developed for PET imaging of integrin $\alpha_v\beta_3$ [6, 7]. The positron emitter ^{18}F-fluoride has a physical half-life of 109.7 min which matches well with in vivo biological half-lives of many bioligands. ^{18}F also has almost 100% positron efficiency and is readily available from a medical cyclotron. Thus, it has been extensively used as a radiolabel for PET imaging [8]. However, most ^{18}F labeling procedures for peptides suffer from lengthy and tedious multistep radiosynthetic procedures. For example, ^{18}F-galacto-RGD that has been evaluated in human subjects requires four steps of radiosynthesis and three rounds of radio high performance liquid chromatography (radio-HPLC) purification [9–11]. The synthesis of another ^{18}F-labeled RGD peptide for clinical trials, ^{18}F-AH111585, involves two reaction pots and two radio-HPLC purifications [12–14]. A few other methods have been reported for radiofluorination of RGD peptides, including amide bond formation using *N*-succinimidyl 4-^{18}F-fluorobenzoate (^{18}F-SFB) [15], oxime formation between aminooxy-functionalized RGD peptides and 4-^{18}F-fluorobenzaldehyde (^{18}F-FBA) [16], and thiol reactive *N*-[2-(4-^{18}F-fluorobenzamido)ethyl]maleimide (^{18}F-FBEM) for RGD monomer and dimer labeling [17]. All of these ^{18}F radiolabeling strategies require multiple reaction steps. Moreover, it is very challenging to make these radiosynthetic processes fully automatic, which in turn sets a high technical barrier for using these PET probes in the clinical setting.

Very recently, a few pioneering studies on one-step ^{18}F labeling methods have been reported, based on fluorine-silicon chemistry [18, 19], fluorine-boron chemistry [20], and 1,4,7-triazacyclononane-1,4,7-triacetic acid (NOTA)-AlF chelation chemistry [21–23]. However, so far none of these methods has been applied in developing RGD-based PET probes for tumor angiogenesis imaging. For radiofluorination strategies involving the NOTA-AlF chelation chemistry and fluorine-boron chemistry, the labeling procedure can be accomplished in water. From a biological perspective, these one-step and water-compatible reactions are ideal for incorporation of ^{18}F-fluoride into biologically active ligands, especially biomacromolecules that are only soluble in water. In this study, we conjugated a dimeric cyclic RGD peptide, E[*c*(RGDyK)]$_2$ (abbreviated as RGD$_2$) with the NOTA chelator to prepare NOTA-RGD$_2$ (Fig. 1a, b). This bioconjugate was then labeled with ^{18}F in one step via the simple ^{18}F-AlF chelation reaction in aqueous phase (Fig. 1c). The synthesized PET probe, ^{18}F-AlF-NOTA-RGD$_2$, was further evaluated in integrin-positive U87MG tumor-bearing mice, and the in vivo performance of ^{18}F-AlF-NOTA-RGD$_2$ was also compared with 4-nitrophenyl 2-^{18}F-fluoropropionate (^{18}F-NFP)-labeled RGD$_2$ (^{18}F-FP-RGD$_2$) that requires two-pot and four-step radiosynthesis.

Materials and methods

All chemicals obtained commercially were of analytical grade and used without further purification. No-carrier-added ^{18}F-fluoride was obtained from an in-house PETtrace cyclotron (GE Healthcare). Reverse-phase extraction C18 Sep-Pak cartridges were obtained from Waters (Milford, MA, USA) and were pretreated with ethanol and water before use. The syringe filter and polyethersulfone membranes (pore size 0.22 μm, diameter 13 mm) were obtained from Nalge Nunc International (Rochester, NY, USA). ^{125}I-Echistatin was purchased from PerkinElmer (Piscataway, NJ, USA). The *c*(RGDyK) and dimeric E[*c*(RGDyK)]$_2$ were obtained from Peptides International (Louisville, KY, USA). The semi-preparative reverse-phase HPLC using a Vydac protein and peptide column (218TP510; 5

μm, 250×10 mm) was performed on a Dionex 680 chromatography system with a UVD 170U absorbance detector (Sunnyvale, CA, USA) and model 105S single-channel radiation detector (Carroll & Ramsey Associates, Berkeley, CA, USA). With a flow rate of 4 ml/min, the mobile phase stayed at 97% solvent A [0.1% trifluoroacetic acid (TFA) in water] and 3% B [0.1% TFA in acetonitrile (MeCN)] at 0–5 min and was changed from 85% solvent A and 15% B at 5 min to 20% solvent A and 80% solvent B at 35 min. Analytical HPLC had the flow rate of 1 ml/min with a Vydac protein and peptide column (218TP510; 5 μm, 250×4.6 mm). The mobile phase gradient was changed from 95% solvent A and 5% B (0–2 min) to 35% solvent A and 65% solvent B at 32 min. The recorded data were processed using Chromeleon version 6.50 software. The UV absorbance was monitored at 218 nm and the identification of the peptides was confirmed based on the UV spectrum using a photodiode array (PDA) detector.

MicroPET scans were performed on a microPET R4 rodent model scanner (Siemens Medical Solutions USA, Inc., Knoxville, TN, USA). The scanner has a computer-controlled bed and 10.8-cm transaxial and 8-cm axial fields of view (FOVs). It has no septa and operates exclusively in the three-dimensional (3-D) list mode. Animals were placed near the center of the FOV of the scanner.

Preparation of NOTA-RGD_2

The chelator, NOTA, was purchased from CheMatch, France. It was activated by 1-ethyl-3-[3-(dimethylamino)propyl] carbodiimide (EDC) and *N*-hydroxysulfono-succinimide (SNHS) and conjugated with RGD_2 as reported earlier (Fig. 1b) [24]. The NOTA-RGD_2 conjugate was purified by a semi-preparative HPLC and characterized by analytical HPLC and matrix-assisted laser desorption/ionization time-of-flight mass spectrometry (MALDI-TOF MS). The retention time (Rt) of the purified peptide was found to be 15.6 min, and the molecular mass was measured to be 1,637.6 for $[M+H]^+$ (chemical formula: $C_{71}H_{107}N_{22}O_{23}$, calculated molecular weight 1,636.7). The synthesis of ^{19}F-AlF-NOTA-RGD_2 followed the published report [23]: analytical HPLC (Rt= 14.7 min) and MALDI-TOF MS: m/z 1,681.2 for $[M]^+$ (chemical formula: $C_{71}H_{106}AlFN_{22}O_{23}$, calculated molecular weight 1,681.7).

Radiochemistry

The ^{18}F labeling reaction is shown in Fig. 1c. A QMA Sep-Pak Light cartridge (Waters, Milford, MA, USA) fixed with 30 mCi (1.1 GBq) of ^{18}F-fluoride was washed with 2.5 ml of metal-free water. ^{18}F was then eluted from the cartridge with 400 μl of 0.4 M $KHCO_3$, from which a 200-μl fraction was taken. The pH of the solution was adjusted to 4 with metal-free glacial acetic acid. $AlCl_3$ (2 mM, 3 μl) in 0.1 M sodium acetate buffer (pH 4) and 5 μl of NOTA-RGD_2 [60 mg/ml in dimethyl sulfoxide (DMSO)] were then added to the reaction solution sequentially. The reaction mixture was incubated at 100°C for 15 min. After dilution with 1 ml of metal-free water, the crude mixture was purified with a semi-preparative HPLC. The fractions containing ^{18}F-AlF-NOTA-RGD_2 were collected and combined and the solvents were removed using a rotary evaporator. The product was reconstituted in phosphate-buffered saline (PBS, 1×, pH 7.4) and passed through a 0.22-μm Millipore filter into a sterile vial for in vitro and in vivo experiments. As a control

experiment, RGD_2 was labeled with ^{18}F-NFP to make ^{18}F-FP-RGD_2 using the published method [25].

Cell culture

Human glioblastoma cell line U87MG was obtained from the American Type Culture Collection (Manassas, VA, USA) and were cultured in DMEM containing high glucose (GIBCO, Carlsbad, CA, USA), which was supplemented with 10% fetal bovine serum (FBS) and 1% penicillin-streptomycin. The cells were expanded in tissue culture dishes and kept in a humidified atmosphere of 5% CO_2 at 37°C. The medium was changed every other day. A confluent monolayer was detached with 0.05% trypsin-ethylenediaminetetraacetate (EDTA), 0.01 M PBS (pH 7.4), and dissociated into a single-cell suspension for further cell culture.

U87MG cell binding assay

This assay was performed as previously described [26]. Briefly, 2×10^5 U87MG cells were incubated with 0.06 nM ^{125}I-labeled echistatin and varying concentrations of compounds (RGD_2 and ^{19}F-AlF-NOTA-RGD_2) in the integrin binding buffer [IBB, 25 mM Tris pH 7.4, 150 mM NaCl, 2 mM $CaCl_2$, 1 mM $MgCl_2$, 1 mM $MnCl_2$, and 0.1% bovine serum albumin (BSA)] at room temperature for 1 h. The cell-bound radioactivity remaining after washing was determined by gamma counting. IC_{50} values, which are the concentrations of the competing compound required to inhibit 50% of radioligand binding, were determined by nonlinear regression using GraphPad Prism (GraphPad Software, Inc., La Jolla, CA, USA). Experiments were performed with quadruplicate samples.

Mouse serum stability

The in vitro stability of ^{18}F-AlF-NOTA-RGD_2 was evaluated by incubation of 3.7 MBq (100 μCi) of the probe with mouse serum (1 ml) at 37°C. At different time points (0.5, 1, and 2 h), the solution was filtered using a NanoSep 3K centrifuge (Pall Corp., Port Washington, NY, USA) to isolate low molecular weight metabolites. The filtrates were analyzed by a reverse-phase HPLC under analytical conditions detailed above.

Animal biodistribution studies

Animal procedures were performed according to a protocol approved by the Stanford University Institutional Animal Care and Use Committee. Approximately 10×10^6 cultured U87MG cells were suspended in PBS and subcutaneously implanted in the right shoulders of female nude mice purchased from Charles River Laboratory (Wilmington, MA, USA). Tumors were allowed to grow to a size of 0.5–1 cm in diameter (2~3 weeks). For biodistribution studies, the nude mice bearing U87MG xenografts (n=4 for each group) were injected with about 3.7 MBq (100 μCi) of ^{18}F-AlF-NOTA-RGD_2 or ^{18}F-FP-RGD_2 through the tail vein and sacrificed at 2.0 h post-injection (p.i.). The blocking study of ^{18}F-AlF-NOTA-RGD_2 was performed by co-injection of the probe with c(RGDyK) (10 mg/kg body weight) through the tail vein. The tumor and normal organs of interest were removed and weighed, and their radioactivity was measured in a gamma counter. The radioactivity

uptakes in the tumor and normal organs were expressed as a percentage of the injected radioactive dose per gram of tissue (%ID/g).

MicroPET imaging

For dynamic imaging studies, U87MG tumor-bearing mice were injected via the tail vein with approximately 3.7 MBq (100 μCi) of ^{18}F-AlF-NOTA-RGD$_2$ and microPET scans (6×20 s, 8×60 s, 10×150 s, total of 24 frames) were started approximately 2 min after probe injection and were continued for 35 min. For static scans, the mice bearing U87MG xenografts were injected with about 3.7 MBq (100 μCi) of ^{18}F-FP-RGD$_2$ or ^{18}F-AlF-NOTA-RGD$_2$ via the tail vein (n=4 for each group). Similarly, the blocking study was performed by injection of the probe with *c* (RGDyK) (10 mg/kg body weight) through the tail vein (n=4). At 0.5, 1, and 2 h p.i., the mice were anesthetized with isoflurane (5% for induction and 2% for maintenance in 100% O_2) using a knockdown box. With the help of a laser beam attached to the scanner, the mice were placed in the prone position near the center of the FOV of the scanner. The 3-min static scans were then obtained. Images were reconstructed by using a two-dimensional ordered subsets expectation maximization (OSEM) algorithm. No background correction was performed. Regions of interest (ROIs; 5 pixels for coronal and transaxial slices) were drawn over the tumor on decay-corrected whole-body coronal images. The maximum counts per pixel per minute were obtained from the ROI and converted to counts per milliliter per minute by using a calibration constant. With the assumption of a tissue density of 1 g/ml, the ROIs were converted to counts per gram per minute. Image ROI-derived %ID/g values were determined by dividing counts per gram per minute by injected dose. No attenuation correction was performed.

Statistical analysis

Quantitative data are expressed as mean ± SD. Means were compared using one-way analysis of variance (ANOVA) and Student's *t* test; *p* values of<0.05 were considered statistically significant.

Results

Chemistry and radiochemistry

The NOTA-RGD$_2$ was prepared by direct conjugation of RGD$_2$ with activated NOTA in 45% yield (Fig. 1b). Both HPLC and mass spectroscopy were used to confirm the identity of the product. The ^{19}F-AlF-NOTA-RGD$_2$ was also synthesized for cell studies and used as a standard for characterization of its radioactive counterpart in HPLC. As shown in Fig. 2a, NOTA-RGD$_2$ and ^{19}F-AlF-NOTA-RGD$_2$ could be clearly separated by analytical HPLC. For purification of the radioactive product, a difference of 0.6 min on retention time on a semi-preparative HPLC was observed between ^{18}F-AlF-NOTA-RGD$_2$ and the unlabeled peptide (Fig. 2b). The whole radiosynthesis was accomplished within 40 min with a decay-corrected yield of 17.9% and radiochemical purity of more than 95%. The specific activity of purified ^{18}F-AlF-NOTA-RGD$_2$ was calculated as 300–400 mCi/μmol. ^{18}F-FP-RGD$_2$ (Fig. 1d) was synthesized using the published method in 15.4% decay-corrected yield starting with ^{18}F-fluoride [25].

Cell binding assay

The competitive cell binding assay was used to determine the receptor binding affinity of ^{19}F-AlF-NOTA-RGD$_2$ and RGD$_2$ (Fig. 3). Both of these peptides inhibited the binding of ^{125}I-echistatin to U87MG cells in a concentration-dependent manner. The IC$_{50}$ values of RGD$_2$ and ^{19}F-AlF-NOTA-RGD$_2$ were 42±4.1 and 46±4.4 nM (n=4), respectively. The comparable IC$_{50}$ values of ^{19}F-AlF-NOTA-RGD$_2$ and RGD$_2$ suggest that incorporation of the NOTA motif has a minimal effect on the RGD$_2$ receptor binding affinity.

Serum stability

^{18}F-AlF-NOTA-RGD$_2$ displayed good stability in mouse serum (Fig. 4). After incubation in serum, more than 95% activity (decay corrected) was recovered for HPLC analysis. The percentage of intact probes remained more than 95% after 0.5, 1, and 2 h incubation in mouse serum at 37°C. Defluorination was not observed for the probe incubated with mouse serum up to 2 h. Overall, ^{18}F-AlF-NOTA-RGD$_2$ could be reliably produced and demonstrated good in vitro stability.

MicroPET imaging studies

The in vivo pharmacokinetic profile and tumor targeting property of ^{18}F-AlF-NOTA-RGD in U87MG tumor-bearing nude mice were evaluated by 35-min dynamic microPET scans followed by static scans at 1 and 2 h p.i. As shown in Fig. 5a, the probe was rapidly cleared from the renal system as determined by ROI analysis of the kidneys. At the first 3 min after tail vein injection, radioactivity rapidly accumulated in kidneys (31.1±4.3%ID/g) but decreased to 10.5±0.5%ID/g at 10 min p.i. In contrast, tumor uptake peaked (5.3±1.2%ID/g) at a very early time point (3 min p.i.) and was maintained throughout the whole dynamic scan frames. Low levels of liver and muscle uptakes were also observed (Fig. 5a).

Representative decay-corrected coronal images of static scans at different time points after injection are shown in Fig. 5b. The U87MG tumors were clearly visualized with good tumor to background contrast for both ^{18}F-AlF-NOTA-RGD$_2$ and ^{18}F-FP-RGD$_2$. For ^{18}F-AlF-NOTA-RGD$_2$, the tumor uptake was 5.7±2.1, 5.3±1.7, and 1.9±0.7%ID/g at 0.5, 1, and 2 h p.i., respectively (Fig. 5c). For ^{18}F-FP-RGD$_2$, the tumor uptake was 4.0±1.1, 2.8±0.7, and 1.1±0.2%ID/g at 0.5, 1, and 2 h p.i., respectively (Fig. 5e). At 1 h p.i., the tumor uptake of ^{18}F-AlF-NOTA-RGD$_2$ is significantly higher than that of ^{18}F-FP-RGD$_2$ (p<0.05). Both of the radiolabeled probes were excreted mainly through the kidneys. Liver, kidney, and muscle uptakes of ^{18}F-AlF-NOTA-RGD$_2$ and ^{18}F-FP-RGD$_2$ had no significant difference (p >0.05) at 2 h p.i. in the static scans.

The microPET images at 0.5, 1, and 2 h p.i. of U87MG tumor-bearing mice injected with ^{18}F-AlF-NOTA-RGD$_2$ and a blocking dose of c(RGDyK) are shown in Fig. 5b. The U87MG tumor uptake was reduced to the background level and the uptake values were 0.46±0.05, 0.29±0.05, and 0.14± 0.09%ID/g at 0.5, 1, and 2 h p.i., respectively, confirming the integrin $\alpha_v\beta_3$-specific targeting of ^{18}F-AlF-NOTA-RGD$_2$ in the integrin-positive U87MG tumor. The uptakes in most of the normal organs (e.g., liver, kidneys, and muscle) were also lower than those without co-injection of c(RGDyK) (Fig. 5d). These results are consistent with previous literature, which is contributed by the expression of integrin

receptors in many normal tissues [30, 31]. Moreover, the reduced uptake of the probe in normal organs might also be caused by the potential toxicity effect of a large dose of *c*(RGDyK).

The tumor to normal organ ratios of ^{18}F-AlF-NOTA-RGD$_2$ and ^{18}F-FP-RGD$_2$ were also calculated for comparison of their in vivo properties at 2 h p.i. (Fig. 5f). Although ^{18}F-AlF-NOTA-RGD$_2$ had higher tumor uptakes than those of ^{18}F-FP-RGD$_2$, the tumor to normal organ ratios showed no significant difference for these two probes (p>0.05).

Biodistribution studies

To validate microPET quantifications, we also performed a biodistribution experiment by directly sampling tumors and normal organs of U87MG tumor-bearing mice 2 h after tail vein injection of ^{18}F-AlF-NOTA-RGD$_2$, ^{18}F-AlF-NOTA-RGD$_2$ with *c*(RGDyK) as blocking agent, and ^{18}F-FP-RGD$_2$ (~100 μCi/mouse). The results are shown in Fig. 6. The tumor uptakes for ^{18}F-AlF-NOTA-RGD$_2$ and ^{18}F-FP-RGD$_2$ were 2.3±0.9 and 1.3±0.8%ID/g, respectively. Except for liver and kidneys, the uptake values in the other major organs for both ^{18}F-AlF-NOTA-RGD$_2$ and ^{18}F-FP-RGD$_2$ were less than 1%ID/g. Of note, the bone uptake of ^{18}F-AlF-NOTA-RGD$_2$ was only 0.53±0.14%ID/g, which is consistent with its high stability in mouse serum. For the blocking study, a decrease of radioactivity was observed in all dissected tissues and organs (black bars in Fig. 6) with the change of tumor uptake being the most significant, as it was reduced markedly from 2.26±0.91 to 0.18±0.02%ID/g at 2 h p.i.

Discussion

The armamentarium of ^{18}F and other radionuclide-labeled RGD peptides for PET imaging of tumor angiogenesis has expanded exponentially in the last decade. Two prominent amino-specific prosthetic agents, ^{18}F-NFP and ^{18}F-SFB, have been widely used for labeling RGD peptides and a variety of applications have been achieved by these two labeling methods. However, to obtain the final radiofluorinated product multiple radiosynthetic steps are almost always required. As a result, the complex radiosynthesis has become a major challenge for automation and subsequently a significant barrier for large-scale and high-radioactivity production for clinical translation. Even the most current ^{18}F-labeled RGD peptides being evaluated in clinics suffer from the laborious radiolabeling procedures [27]. Therefore, the recently reported novel ^{18}F labeling methods [20–23, 28] inspired us to pursue a straightforward, single-step, and powerful labeling strategy to radiofluorinate RGD peptides for future preclinical and clinical applications. In this study, we explored the ^{18}F-AlF-NOTA labeling method pioneered by McBride et al. [23] and evaluated our product ^{18}F-AlF-NOTA-RGD$_2$ in U87MG tumor-bearing mice.

Using the published optimal reaction condition [21], we radiofluorinated NOTA-RGD$_2$ with 17.9% decay-corrected yield within 40 min after bombardment. Figure 2b shows the semi-preparative HPLC result for the purification of the final product. The ^{18}F-labeled NOTA-RGD$_2$ is eluted at 12.5 min, while the unlabeled NOTA-RGD$_2$ is washed out at 13.1 min. The good separation of the unlabeled precursor from the PET probe results in the high specific activity of ^{18}F-AlF-NOTA-RGD$_2$. Of note, in the published literature two rapid

interchangeable isomers that accounted for the ^{18}F-labeled products were obtained [21–23]. However, in our study only one radiolabeled product was observed, presumably because a different peptide was used for radiosynthesis.

Among all the ^{18}F-labeled RGD peptides reported so far, at least one round of azeotropic drying is needed in the whole synthesis scheme. This step requires high-quality drying instruments and good techniques from radiochemists. Failure to dry ^{18}F-fluoride properly could result in low yields or even no product. With the ^{18}F-AlF-NOTA labeling method, however, water is used as the solvent for reaction and thus the drying step is no longer necessary, which is a significant advantage over conventional methods and makes this method of ^{18}F labeling of RGD peptides even more robust and attractive.

The ^{18}F-AlF-NOTA-RGD$_2$ was first evaluated by dynamic microPET in the U87MG glioblastoma xenograft mouse model, which has been well established to have a high integrin $\alpha_v\beta_3$ expression [29]. The probe showed prominent uptake in the tumor and a predominant renal clearance. On a side-by-side comparison with ^{18}F-labeled dimeric RGD using conventional ^{18}F-NFP synthon, higher tumor uptakes could be observed for ^{18}F-AlF-NOTA-RGD$_2$ at 0.5 and 1 h p.i. than those of ^{18}F-FP-RGD$_2$ at the same time points ($p<0.05$). However, similar tumor to normal organ ratios were obtained for the two probes despite the statistically significant difference in uptake values of the tumor (Fig. 5f). The results of the biodistribution study demonstrate that both ^{18}F-AlF-NOTA-RGD$_2$ and ^{18}F-FP-RGD$_2$ show a high tumor uptake at 2 h p.i., which further validates the PET quantification. These results highlight that the ^{18}F-AlF-NOTA-RGD$_2$ probe is as good as the ^{18}F-FP-RGD$_2$ labeled with the well-developed ^{18}F-NFP synthon. Furthermore, the Al^{18}F-NOTA moiety does not compromise the in vivo tumor targeting ability of RGD$_2$, given both the in vitro serum stability results and the aforementioned in vivo data. The very low uptake of the bone of the Al^{18}F-NOTA complex further validates the compound's excellent stability in vivo. Most importantly, the true advantage of the labeling method of RGD peptides reported in this study lies in its efficiency. Taking into consideration the conventional four-step and two-pot radiosynthesis of ^{18}F-FP-RGD$_2$ and its minimum 2-h reaction time, the novel RGD labeling method is not only simpler but also significantly faster with its one-step synthesis and 40-min production time. The success of this single-step, good-yield, and easy-operation protocol for production of ^{18}F-AlF-NOTA-RGD$_2$ warrants further applications in labeling a variety of other biomolecules. For now, it can serve as a very promising labeling approach for preparation of RGD-based PET probes and can facilitate the translation of these probes into clinical applications.

Conclusion

NOTA-RGD$_2$ conjugate was successfully prepared and radiolabeled with ^{18}F-fluoride via Al^{18}F intermediate with good yield. This fluorination method for the RGD peptide was very simple and straightforward and the labeled product ^{18}F-AlF-NOTA-RGD$_2$ exhibits excellent in vitro serum stability and in vivo tumor imaging properties. The favorable in vivo performance and the easy production method of ^{18}F-AlF-NOTA-RGD$_2$ warrant further optimization of this probe as well as the radiofluorination strategy so that the clinical translation of ^{18}F-labeled RGD peptides can be accelerated.

Acknowledgments

This work was supported, in part, by NCI 5R01 CA119053 (ZC) and In vivo Cellular Molecular Imaging Center (ICMIC) grant P50 CA114747 (SSG).

References

1. Brooks PC, Montgomery AM, Rosenfeld M, Reisfeld RA, Hu T, Klier G, et al. Integrin αvβ3 antagonists promote tumor regression by inducing apoptosis of angiogenic blood vessels. Cell. 1994; 79:1157–64. [PubMed: 7528107]
2. Chiang AC, Massagué J. Molecular basis of metastasis. N Engl J Med. 2008; 359:2814–23. [PubMed: 19109576]
3. Klein CA. Cancer. The metastasis cascade. Science. 2008; 321:1785–7. [PubMed: 18818347]
4. Podsypanina K, Du YC, Jechlinger M, Beverly LJ, Hambardzumyan D, Varmus H. Seeding and propagation of untransformed mouse mammary cells in the lung. Science. 2008; 321:1841–4. [PubMed: 18755941]
5. Kumar CC. Integrin αvβ3 as a therapeutic target for blocking tumor-induced angiogenesis. Curr Drug Targets. 2003; 4:123–31. [PubMed: 12558065]
6. Jacobson O, Zhu L, Niu G, Weiss ID, Szajek LP, Ma Y, et al. MicroPET imaging of integrin α(v)β(3) expressing tumors using (89)Zr-RGD peptides. Mol Imaging Biol. 2010
7. Haubner R, Beer AJ, Wang H, Chen X. Positron emission tomography tracers for imaging angiogenesis. Eur J Nucl Med Mol Imaging. 2010; 37 (Suppl 1):S86–103. [PubMed: 20559632]
8. Coenen HH, Elsinga PH, Iwata R, Kilbourn MR, Pillai MR, Rajan MG, et al. Fluorine-18 radiopharmaceuticals beyond [18F]FDG for use in oncology and neurosciences. Nucl Med Biol. 2010; 37:727–40. [PubMed: 20870148]
9. Haubner R, Wester HJ, Weber WA, Mang C, Ziegler SI, Goodman SL, et al. Noninvasive imaging of αvβ3 integrin expression using 18F-labeled RGD-containing glycopeptide and positron emission tomography. Cancer Res. 2001; 61:1781–5. [PubMed: 11280722]
10. Beer AJ, Haubner R, Goebel M, Luderschmidt S, Spilker ME, Wester HJ, et al. Biodistribution and pharmacokinetics of the αvβ3-selective tracer 18F-galacto-RGD in cancer patients. J Nucl Med. 2005; 46:1333–41. [PubMed: 16085591]
11. Haubner R, Weber WA, Beer AJ, Vabuliene E, Reim D, Sarbia M, et al. Noninvasive visualization of the activated αvβ3 integrin in cancer patients by positron emission tomography and [18F]Galacto-RGD. PLoS Med. 2005; 2:e70. [PubMed: 15783258]
12. Morrison MS, Ricketts SA, Barnett J, Cuthbertson A, Tessier J, Wedge SR. Use of a novel Arg-Gly-Asp radioligand, 18F-AH111585, to determine changes in tumor vascularity after antitumor therapy. J Nucl Med. 2009; 50:116–22. [PubMed: 19091899]
13. McParland BJ, Miller MP, Spinks TJ, Kenny LM, Osman S, Khela MK, et al. The biodistribution and radiation dosimetry of the Arg-Gly-Asp peptide 18F-AH111585 in healthy volunteers. J Nucl Med. 2008; 49:1664–7. [PubMed: 18794263]
14. Kenny LM, Coombes RC, Oulie I, Contractor KB, Miller M, Spinks TJ, et al. Phase I trial of the positron-emitting Arg-Gly-Asp (RGD) peptide radioligand 18F-AH111585 in breast cancer patients. J Nucl Med. 2008; 49:879–86. [PubMed: 18483090]
15. Wu Z, Li ZB, Cai W, He L, Chin FT, Li F, et al. 18F-labeled mini-PEG spacered RGD dimer (18F-FPRGD2): synthesis and microPET imaging of αvβ3 integrin expression. Eur J Nucl Med Mol Imaging. 2007; 34:1823–31. [PubMed: 17492285]
16. Poethko T, Schottelius M, Thumshirn G, Hersel U, Herz M, Henriksen G, et al. Two-step methodology for high-yield routine radiohalogenation of peptides: (18)F-labeled RGD and octreotide analogs. J Nucl Med. 2004; 45:892–902. [PubMed: 15136641]
17. Cai W, Zhang X, Wu Y, Chen X. A thiol-reactive 18F-labeling agent, N-[2-(4-18F-fluorobenzamido)ethyl]maleimide, and synthesis of RGD peptide-based tracer for PET imaging of αvβ3 integrin expression. J Nucl Med. 2006; 47:1172–80. [PubMed: 16818952]

18. Höhne A, Mu L, Honer M, Schubiger PA, Ametamey SM, Graham K, et al. Synthesis, 18F-labeling, and in vitro and in vivo studies of bombesin peptides modified with silicon-based building blocks. Bioconjug Chem. 2008; 19:1871–9. [PubMed: 18754574]
19. Höhne A, Yu L, Mu L, Reiher M, Voigtmann U, Klar U, et al. Organofluorosilanes as model compounds for 18F-labeled silicon-based PET tracers and their hydrolytic stability: experimental data and theoretical calculations (PET=positron emission tomography). Chemistry. 2009; 15:3736–43. [PubMed: 19267382]
20. Ting R, Harwig C, auf dem Keller U, McCormick S, Austin P, Overall CM, et al. Toward [18F]-labeled aryltrifluoroborate radiotracers: in vivo positron emission tomography imaging of stable aryltrifluoroborate clearance in mice. J Am Chem Soc. 2008; 130:12045–55. [PubMed: 18700764]
21. Laverman P, McBride WJ, Sharkey RM, Eek A, Joosten L, Oyen WJ, et al. A novel facile method of labeling octreotide with (18)F-fluorine. J Nucl Med. 2010; 51:454–61. [PubMed: 20150268]
22. McBride WJ, D'Souza CA, Sharkey RM, Karacay H, Rossi EA, Chang CH, et al. Improved 18F labeling of peptides with a fluoride-aluminum-chelate complex. Bioconjug Chem. 2010; 21:1331–40. [PubMed: 20540570]
23. McBride WJ, Sharkey RM, Karacay H, D'Souza CA, Rossi EA, Laverman P, et al. A novel method of 18F radiolabeling for PET. J Nucl Med. 2009; 50:991–8. [PubMed: 19443594]
24. Wu Y, Zhang X, Xiong Z, Cheng Z, Fisher DR, Liu S, et al. microPET imaging of glioma integrin αvβ3 expression using (64) Cu-labeled tetrameric RGD peptide. J Nucl Med. 2005; 46:1707–18. [PubMed: 16204722]
25. Liu S, Liu Z, Chen K, Yan Y, Watzlowik P, Wester HJ, et al. 18F-labeled galacto and PEGylated RGD dimers for PET imaging of αvβ3 integrin expression. Mol Imaging Biol. 2010; 12:530–8. [PubMed: 19949981]
26. Cheng Z, Wu Y, Xiong Z, Gambhir SS, Chen X. Near-infrared fluorescent RGD peptides for optical imaging of integrin αvβ3 expression in living mice. Bioconjug Chem. 2005; 16:1433–41. [PubMed: 16287239]
27. Mittra E, Goris ML, Lagaru AH, Kardan A, Burton L, Berganos R, et al. Pilot pharmacokinetic and dosimetric studies of [18F] FPPRGD2: a PET radiopharmaceutical agent for imaging αvβ3 integrin levels. Radiology. 2011 In press.
28. de Bruin B, Kuhnast B, Hinnen F, Yaouancq L, Amessou M, Johannes L, et al. 1-[3-(2-[18F]fluoropyridin-3-yloxy)propyl] pyrrole-2,5-dione: design, synthesis, and radiosynthesis of a new [18F]fluoropyridine-based maleimide reagent for the labeling of peptides and proteins. Bioconjug Chem. 2005; 16:406–20. [PubMed: 15769096]
29. Jiang L, Kimura RH, Miao Z, Silverman AP, Ren G, Liu H, et al. Evaluation of a (64)Cu-labeled cystine-knot peptide based on agouti-related protein for PET of tumors expressing αvβ3 integrin. J Nucl Med. 2010; 51:251–8. [PubMed: 20124048]
30. Chen X, Park R, Tohme M, Shahinian AH, Bading JR, Conti PS. MicroPET and autoradiographic imaging of breast cancer alpha v-integrin expression using 18F- and 64Cu-labeled RGD peptide. Bioconjug Chem. 2004; 15:41–9. [PubMed: 14733582]
31. Li ZB, Cai W, Cao Q, Chen K, Wu Z, He L, et al. (64)Cu-labeled tetrameric and octameric RGD peptides for small-animal PET of tumor αvβ3 integrin expression. J Nucl Med. 2007; 48:1162–71. [PubMed: 17574975]

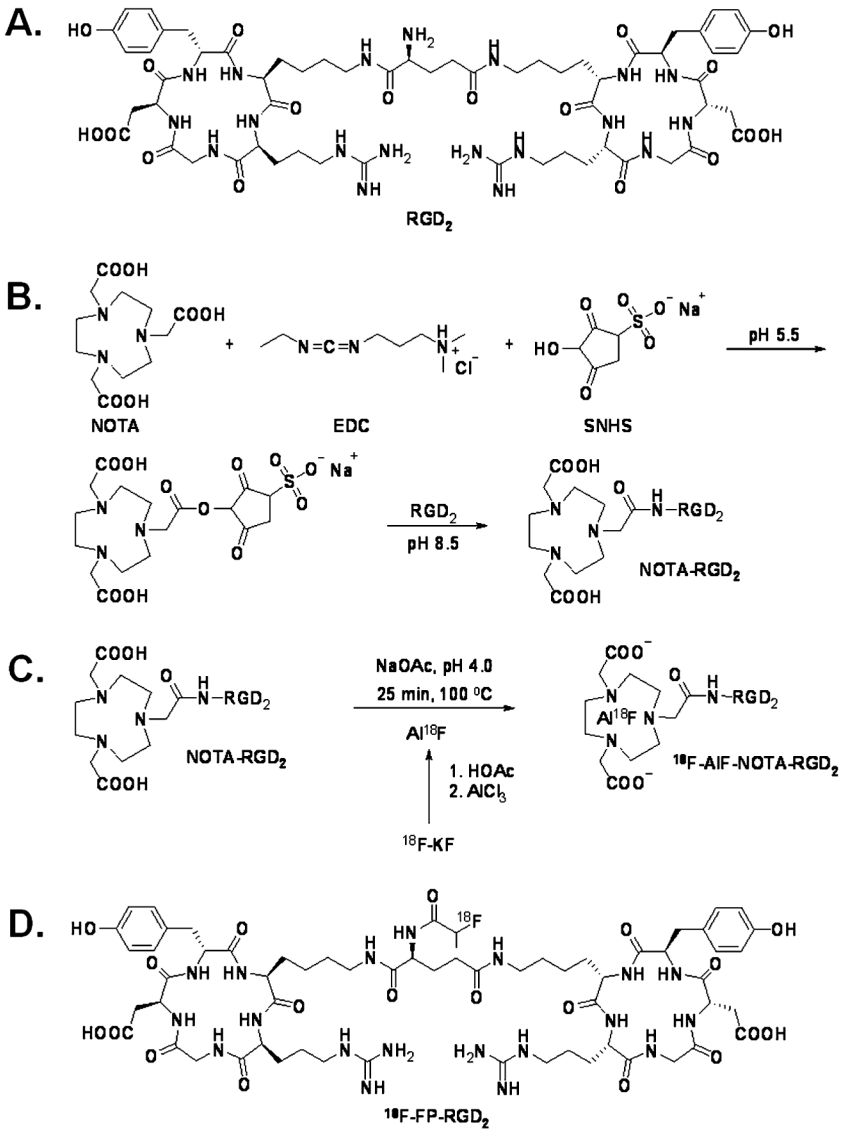

Fig. 1.

a Schematic structure of peptide RGD_2. **b** The synthesis of NOTA-RGD_2 from RGD_2. **c** The ^{18}F labeling of NOTA-RGD_2 to ^{18}F-AlF-NOTA-RGD_2. **d** The structure of ^{18}F-FP-RGD_2

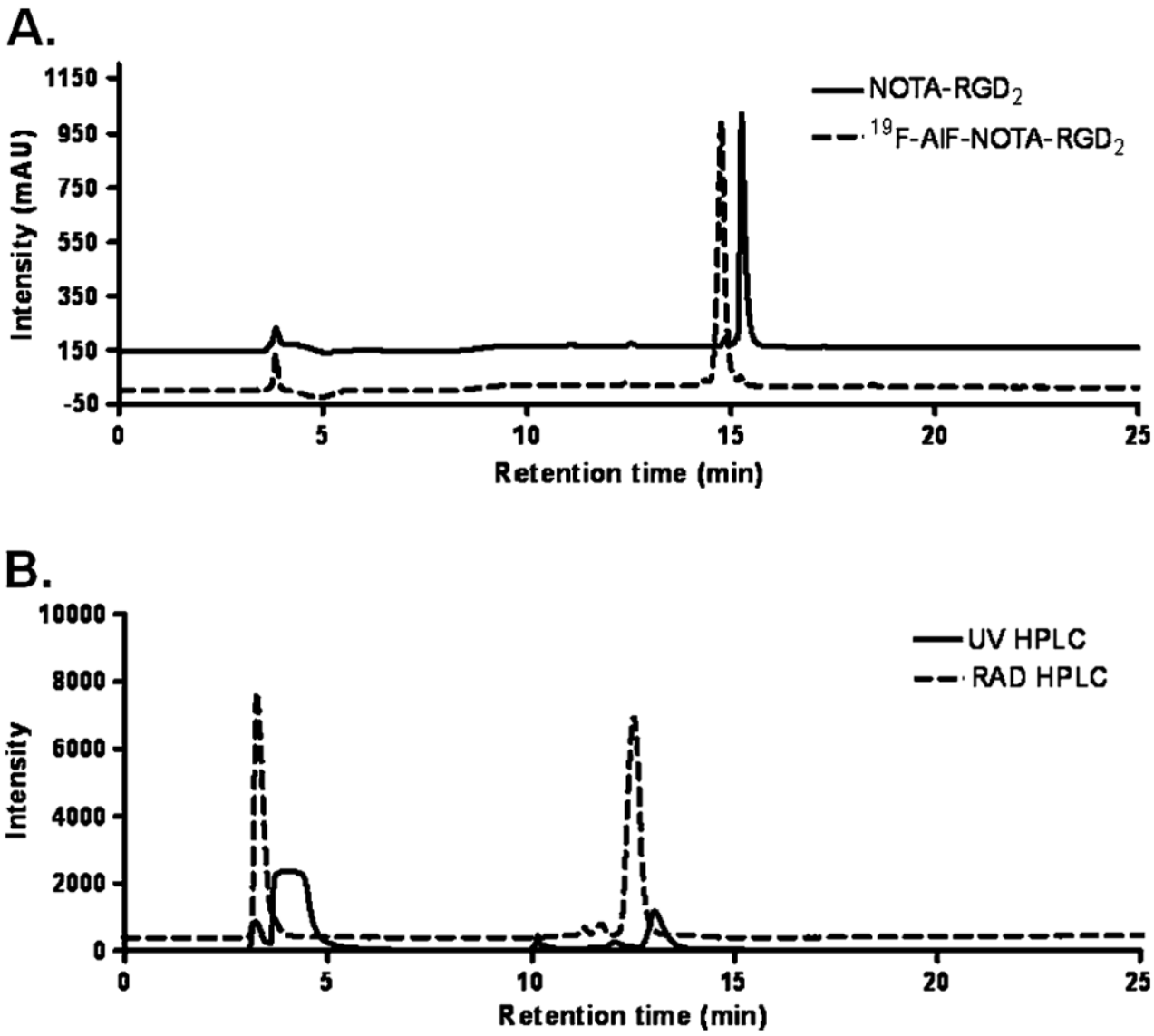

Fig. 2.

a The analytical HPLC for NOTA-RGD_2 (*solid line*) and ^{19}F-AlF-NOTA-RGD_2 (*dotted line*). **b** HPLC chromatograms of ^{18}F-AlF-NOTA-RGD_2 purification. The relative intensity of UV was expressed as milli-absorbance unit (mAU) and RAD signals were expressed as millivolt (mV)

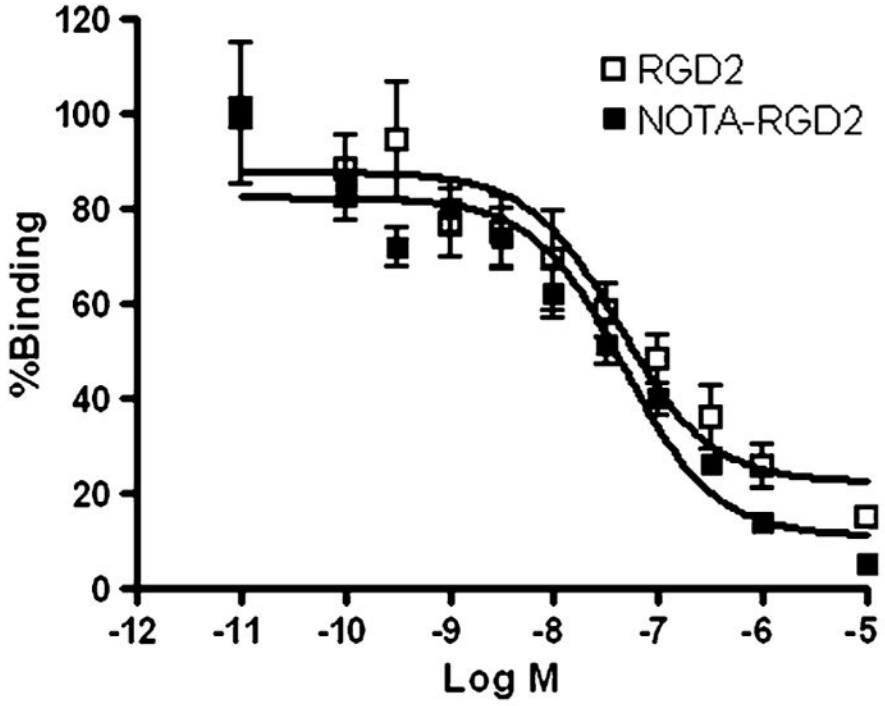

Fig. 3.

Inhibition of ^{125}I-echistatin binding to integrin $\alpha_v\beta_3$ on U87MG cells by RGD_2 and ^{19}F-AlF-NOTA-RGD_2 (n=4, mean ± SD)

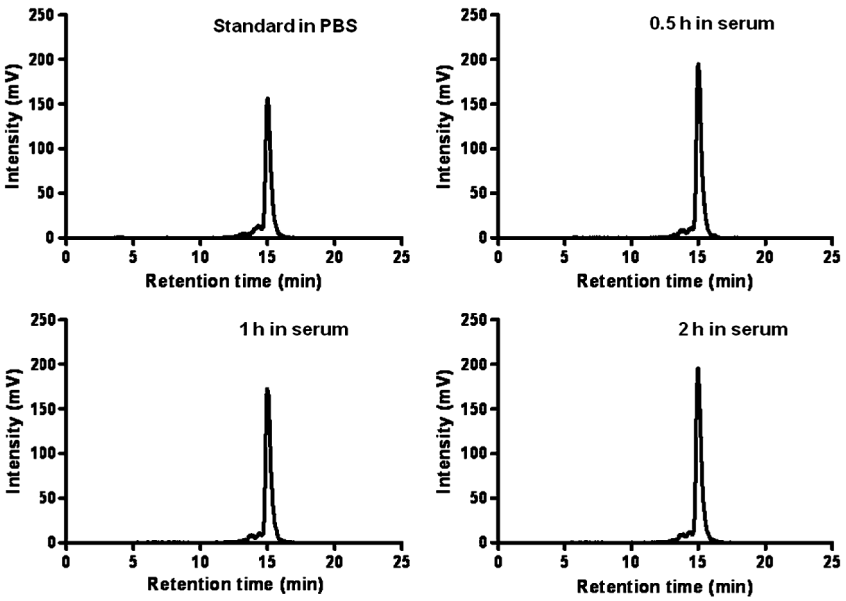

Fig. 4.

^{18}F-AlF-NOTA-RGD$_2$ stability in mouse serum after incubation at 37°C for 0.5, 1, and 2 h

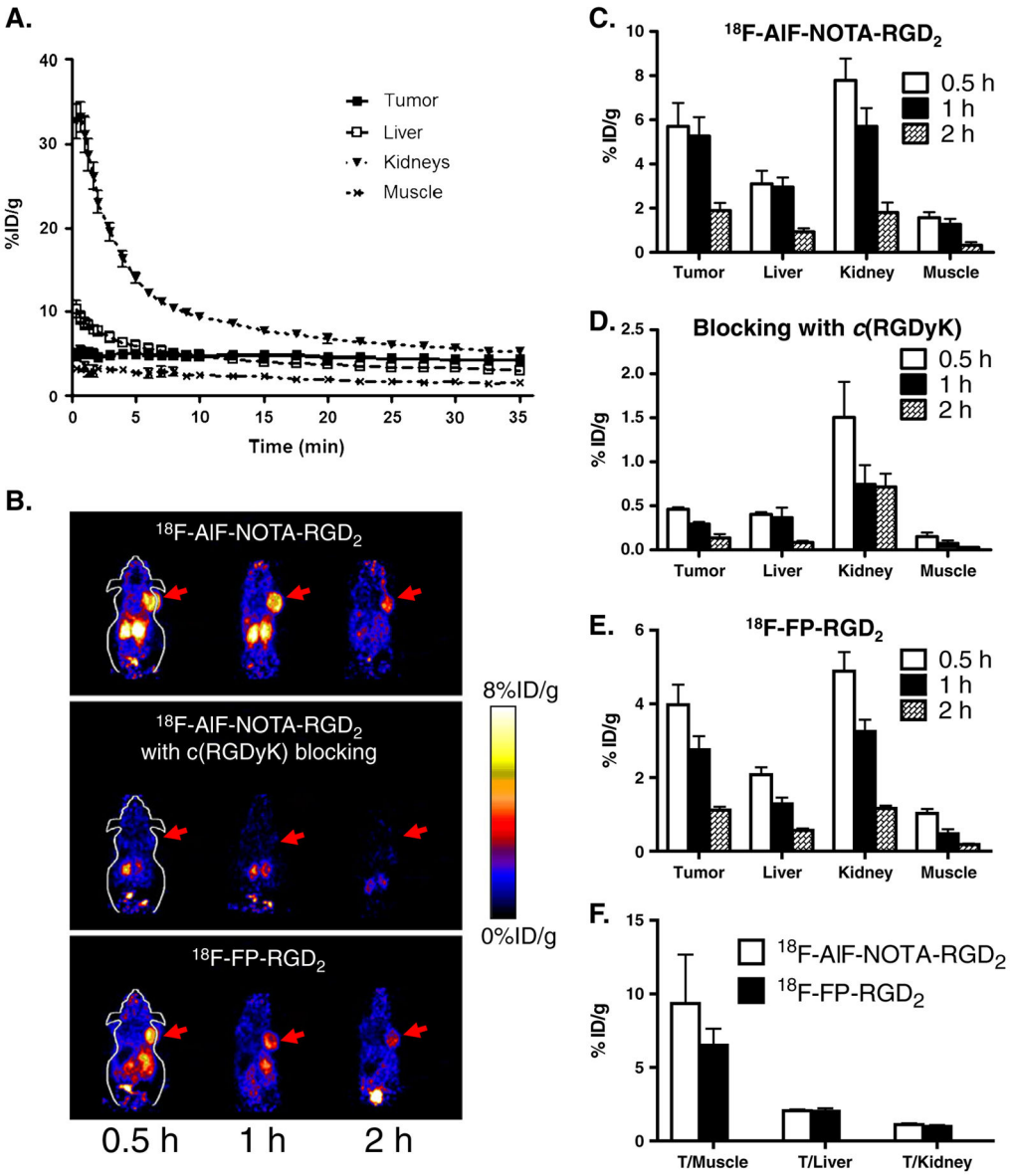

Fig. 5.

a Time-activity curves of tumor and major organs of athymic female nude mice bearing U87MG tumor from 35-min dynamic scans after intravenous injection of ^{18}F-AlF-NOTA-RGD$_2$ (~100 μCi/mouse, n=4). **b** Decay-corrected whole-body coronal microPET images of athymic female nude mice bearing U87MG tumor from a static scan at 0.5, 1, and 2 h after injection of ^{18}F-AlF-NOTA-RGD$_2$, ^{18}F-AlF-NOTA-RGD$_2$ with *c*(RGDyK) as blocking agent (10 mg/kg body weight), and ^{18}F-FP-RGD2. Tumors are indicated by *arrows*. **c**–**e** MicroPET quantification of tumors and major organs at 0.5, 1, and 2 h after injection of ^{18}F-AlF-NOTA-RGD$_2$, ^{18}F-AlF-NOTA-RGD$_2$ with RGD as blocking (10 mg/kg body weight), and ^{18}F-FP-RGD$_2$, respectively. **f** Comparison of tumor to normal organ/tissue (muscle, kidney, liver) ratios of ^{18}F-AlF-NOTA-RGD$_2$ and ^{18}F-FP-RGD$_2$ at 2 h p.i.

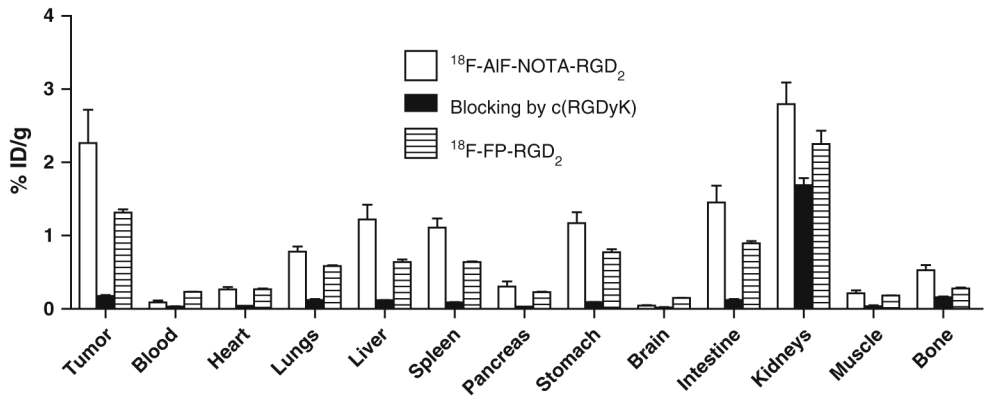

Fig. 6.

Biodistributions of ^{18}F-AlF-NOTA-RGD$_2$, ^{18}F-AlF-NOTA-RGD$_2$ with *c*(RGDyK) as a blocking agent (10 mg/kg body weight), and ^{18}F-FP-RGD$_2$ in U87MG tumor-bearing athymic nude mice at 2 h p.i. Data are expressed as normalized accumulation of activity in %ID/g ± SD (*n*=4)